Journal of Applied Polymer Science

Adhesion Properties of Soy Protein Crosslinked with Organic Calcium Silicate Hydrate Hybrids

Min Jung Kim, Xiuzhi Susan Sun
Department of Grain Science and Industry, Bio-Materials and Technology Laboratory, Kansas State University, Manhattan Kansas, 66506
Correspondence to: X. S. Sun (E-mail: xss@k-state.edu)

ABSTRACT: The objective of this work was to investigate if inorganic calcium silicate hydrate (CSH) hybrids would improve soy protein wet adhesion properties. 3-aminopropyltriethoxysilane (APTES) was used as a crosslinking agent to make covalent linkage between organic soy protein and inorganic CSH phases. Soy protein–calcium silicate hydrate (MSP-CSH) composites with different mole ratio of APTES were prepared and the effect of crosslinking reaction on physicochemical properties such as thermal, rheological, FTIR spectroscopic, and morphological and adhesion properties were studied with physical aging effect. Covalent linkage was observed between CSH and soy protein using the FTIR technique. With aging effect, the denaturation temperature (T_d) and enthalpies (ΔH_d) of each fraction of soy protein increased in DSC thermograms, representing higher thermal stability, and the viscoelasticity of the composites also increased. The roughly coated surface of the MSP-CSH composite was observed in SEM images. All these changes further confirmed the interaction between CSH and soy protein molecules. Dry and wet adhesion strength of the MSP-CSH composites was higher than the control MSP alone. © 2014 Wiley Periodicals, Inc. J. Appl. Polym. Sci. **2014**, *131*, 40693.

KEYWORDS: adhesives; biomaterials; biopolymers; renewable polymers

Received 27 January 2014; accepted 9 March 2014
DOI: 10.1002/app.40693

INTRODUCTION

Soy protein consists of two major storage proteins, β-conglycinin (7S), and glycinin (11S), which contribute to the physicochemical properties of soy protein.[1] 7S protein comprises 20–30% of total soy protein with a molecular weight of 175 KDa. It contains α, α', and β polypeptides that are compactly folded together by hydrophobic forces and hydrogen bonding.[2] 11S protein, with a molecular weight 350KDa, makes up 30–50% of total soy protein and has six subunits. Each subunit has a generalized structure of A-SS-B, where A and B represent acidic and basic polypeptides, respectively, linked by a disulfide (SS) bond.[3] Generally, α, α', and acidic polypeptides are regarded as hydrophilic, whereas β and basic polypeptides are considered to be more hydrophobic. Inherent differences in structure and molecular properties of each component of soy protein make them possess different properties such as solubility, thermal properties, and adhesion performance.[4–14]

Polymeric materials, especially those obtained from renewable resources such as natural fibers, have attracted an increasing attention during the last few years due to environmental concerns.[15–20] Particularly, limited petroleum resources and the pollution caused by formaldehyde-based adhesives have spurred many efforts to develop bio-based adhesives with good adhesion properties that can compete with synthetic petroleum-based adhesives. Among them, soy protein-based adhesives have attracted considerable attention as bio-based adhesives since 1930s. Hydrophilic/hydrophobic and charged polypeptide fractions in soy protein can be manipulated to modify surface reactivity and accessibility, which enables soy protein to be applied in the adhesive application. Efforts to improve adhesion properties of soy protein-based adhesives have included using denaturants, reducing agents, and crosslinking agents as well as enzyme hydrolysis.[7,21–26] However, the low water resistance of soy protein based adhesives still limits their extensive applications.[27–29]

Calcium silicate hydrate (CSH) is the main hydrated phases in cement paste and it can be simply synthesized by preparing a mixture of popular silica precursor, tetraethoxysilane (TEOS), and calcium chloride solutions as the starting materials, which procedure has been established by Suzuki.[30] The structure of the prepared inorganic CSH consists of condensed silicate tetraedra sharing oxygen atoms with a central, calcium hydroxide-like CaO_2 sheet.[31] CSH is a main component that contributes to the mechanical strength of cement and a loosely organized binding phase with an associated internal network of micro-sized pores.[14,32–34] Because of its nanocrystalline structure with high

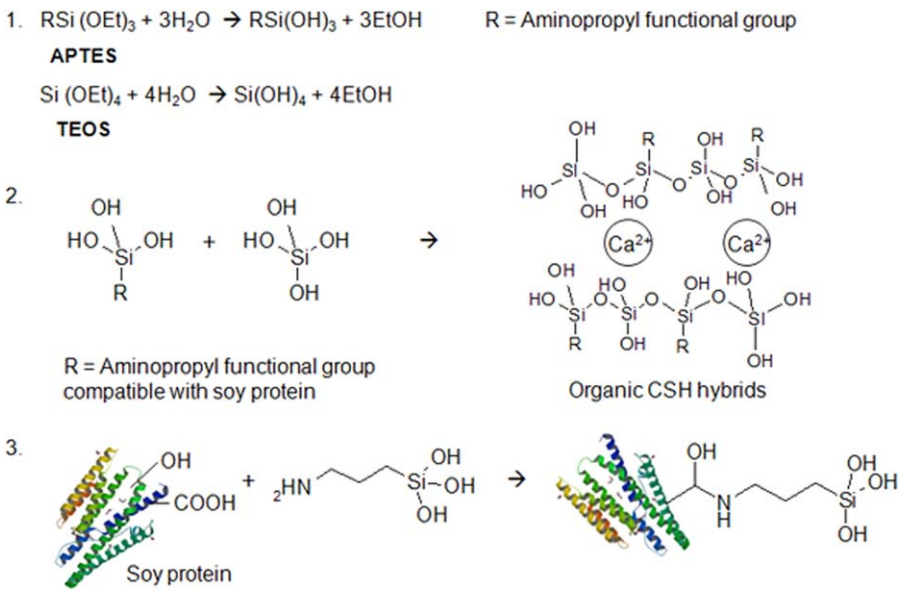

Figure 1. Hypothesis of the reaction pathways between soy protein and CSH at the covalent interface. [Color figure can be viewed in the online issue, which is available at wileyonlinelibrary.com.]

specific surface area[35,36] and bioactivity, it has been a potential to be applied for drug delivery and biomedical applications.[32,33] Minet et al. then introduced the small organic moieties into inorganic CSH phase by using a mixture of two silica precursors, 3-aminopropyltriethoxysilane (APTES), and TEOS that was named organic CSH hybrid.[37] They achieved the successful graft of small aminopropyl molecules to the interlayer domain of inorganic CSH without disrupting their structural integrity, which contribute to reinforced mechanical properties of cement. Their novel approach can provide us with another possibility to fabricate polymer-CSH composite via covalent bridges.

This report focuses on the synthesis and characterization of soy protein–based CSH composites that possess desirable properties for adhesives. We hypothesize that the specific incorporation of CSH into a continuous soy polymeric phases may be achieved by forming covalent bridges between functional groups of soy protein and aminopropyl groups from organic CSH hybrids. This may improve interfacial adhesion strength by accomplishing the inclusion of small inorganic crystallites, the formation of covalent interface, and the reduction of water-sensitive functional groups. To promote the reaction between aminopropyl group of CSH and soy protein, soy protein must be unfolded to expose its functional groups. Considerable attempts have been made to unfold soy protein,[38,39] but they have not been able to overcome the disadvantages such as high viscosity, low concentration of soy protein, and low water resistance.[29,40] Our preliminary studies successfully exploited a new viscous modified soy protein based adhesive by sodium bisulfate (MSP) with high solid content of 38%, good flowability, long shelf life, and good water resistance.[41,42] We strongly believe that this partially unfolded MSP would have advantages over conventional soy protein isolate (SPI), soy flour (SF), and soy concentrate with a native state for adhesive applications. In this work, MSP was used as a base polymer to prepare modified soy protein-CSH (MSP-CSH) composites and the influence of different synthesis parameters on thermal, spectroscopic and mechanical properties of the composite was studied. Especially, we focus on the study of the interfacial crosslinking effect of aminopropyl silane (APTES) on functional properties of MSP-CSH composite.

Reaction Mechanism Hypothesis

The proposed interfacial mechanism governing this experiment is illustrated in Figure 1. Initially, the two silicate precursors APTES and TEOS can be hydrolyzed under acidic conditions, leading to silanol formation in the synthesis of organic CSH hybrids. The silanols from the reaction interact with each other to undergo polycondensation, making very stable siloxane bonds of organic CSH hybrids. During *in-situ* sol–gel polymerization, aminopropyl organic groups of APTES can be incorporated with silicate chains with less than 40% molar ratio, confirming CSH structural integrity.[37] This hybrid materials obtained by the sol–gel method maintain a lamellar structure constituted by an inorganic calcium silicate layer with organic groups confined in the interlayer as shown in the reaction 2 of Figure 1.[30,37]APTES is a molecule that carries two different reactive groups on its silicone atom and as shown in reaction 3 of Figure 1, we assumed that MSP and organic CSH hybrid can be grafted through covalent bridges of APTES. When preparing MSP-CSH composites, aminopropyl group of APTES could react with side chains such as carboxylic acid and hydroxyl groups of soy protein[22] and simultaneously, couple with CSH phases. Upon curing, MSP-CSH composites could form a stable and interconnected structure at the interface. In summary, the introduction of such small crystallite CSH in soy protein would contribute to improved interfacial adhesion through the formation of covalent bridges between soy protein molecules and CSH. Furthermore, we expected to achieve lower surface energy as well as a hydrophobic effect in the presence of nonpolar alkyl groups at the interface, which would result in improved wet shear adhesion. This chemistry strategy has been previously demonstrated by other researchers using other polymers.[22,23,43]

Table I. Sample Information of Organic CSH Hybrids by Varying the Starting Fraction of ATPES with Molar Ratio of 0, 20, and 40% Based on TEOS

In-situ organic CSH hybrid synthesis				
Sample name	Molar ratio of APTES to TEOS	Molar concentration of APTES	Molar concentration of TEOS	Composite Name
CSH	0.0:1.0	0.000	0.606	MSP-CSH
CSH/20% APTES	0.2:0.8	0.121	0.485	MSP-CSH/20% APTES
CSH/40% APTES	0.4:0.6	0.242	0.364	MSP-CSH/40% APTES

This report is the first attempt to examine the potential of inorganic CSH to improve the adhesion properties of soy protein via covalent linkages. To verify this hypothesis, the physicochemical and adhesive properties of MSP-CSH composites with the different synthesis parameter were studied.

EXPERIMENTAL

MSP Sample Preparation

MSP was extracted from soy flour slurry modified with sodium bisulfite using the acid precipitation method described by Qi et al.[41,42] Defatted soy protein flour was dispersed in water at pH 9.5 using 2*N* NaOH. The $NaHSO_3$ (6 g/L) was added to the soy protein slurry and stirred for 2 h. The pH of the slurry was then adjusted to pH 5.4 with 2N HCl to remove carbohydrates by centrifugation at 12,000 × *g*. Then, the pH of the supernatant was adjusted to 4.8 with 2N HCl and centrifuged at 8000 × *g*.

Synthesis of Hybrid Organic CSH and Adhesive Preparation

Organic CSH hybrids were prepared following the sol–gel synthesis method by Minet.[37] Base solution was prepared by dissolving 0.46 g of $CaCl_2$ in 0.1*M* HCl (1.35 cm^3) and ethanol (6.9 cm^3). The mole percentage of APTES relative to the total source of silicon (APTES + TEOS) was varied from 0, 20, and 40%. Different moles of APTES and TEOS were added to the base solution to prepare organic CSH hybrids (Table I). The pure inorganic material (0% APTES, 100% TEOS) is pure CSH as shown in Table I. As APTES increased, the mixture solution rapidly became opaque due to the rapid gelation of silica precursors. At CSH/40% APTES, the mixture solution immediately became cloudy and opaque. The prepared organic CSH hybrids (5 wt % of total weight basis) were thoroughly blended with MSP to fabricate the composites for adhesives. The last column of the Table I includes the information of the composites prepared.

Differential Scanning Calorimetry (DSC)

The thermal denaturation properties of soy proteins were assessed with a differential scanning calorimeter (DSC) (DSC7, Perkin-Elmer, Norwalk, CT) calibrated with indium and zinc. Wet samples of MSP-CSH composites were weighed (15 mg) and hermetically sealed in a large-volume stainless pan. Each sample was held at 30°C for 1 min, then scanned from 20 to 170°C at a heating rate of 10°C/min. Peak temperatures (T_d) and denaturation enthalpies (ΔH_d) were calculated from thermograms.

Dynamic Viscoelastic Measurement

A Bohlin CVOR 150 rheometer (Malvern Instruments, Southborough, MA) was used to characterize the viscoelastic properties of MSP-CSH composites. A parallel plate head was used with 20-mm plate diameter and a 500-μm gap. The measurements were performed in a strain-controlled mode wherein the amplitude of shear strain was 0.01%, and the frequency range was from 0.01 to 25 Hz. The testing temperature was 25°C. A thin layer of silicon oil was spread over the circumference of the sample to prevent dehydration of the samples during test. The elastic modulus (G') and complex viscosity (η) were continuously recorded, and all measurements were triplicated and averaged.

FTIR Spectroscopy

Fourier transform infrared (FTIR) spectra were collected in the region of 4000–650 cm^{-1} with a Perkin-Elmer Spotlight 100 FTIR spectrometer (Waltham, MA). All samples for IR spectroscopic measurement were freeze-dried then ground into powder. Then the samples were made into a disk under the constant force of 30 units. Spectra of the attenuated total reflection (ATR) mode were collected with 128 scans at a resolution of 4 cm^{-1}.

Scanning Electron Microscopy

A Hitachi S-3500 N (Hitachi Science System, Ibaraki, Japan) SEM was used to observe the microstructure of cured MSP-CSH composites. The grounded powder of cured MSP-CSH composite were affixed to an aluminum stub with two-sided tape and coated with an alloy of 60% gold and 40% palladium with a sputter coater (Desk II Sputter/Etch Unit, Moorestown, NJ). The SEM images of the composites were performed with operation conditions at an accelerating voltage of 5 kV.

Two Ply Plywood Specimen Preparation

Cherry wood veneers with dimensions of 50 × 127 × 5 mm^3 were preconditioned in a chamber (Electro-Tech Systems, Glenside, PA) for 7 day at 23°C and 50% relative humidity. The adhesives were brushed onto one end of a piece of cherry wood with dimensions of 127 × 20 mm^2 (length × width) until the entire area was completely wet. Two brushed wood pieces were assembled immediately and conditioned for 10 min at room temperature. Then the assembled wood specimens were pressed with a hot press (Model 3890 Auto M; Carver, Wabash, IN) at 1.4 MPa and 170°C for 10 min.

Three Ply Plywood Specimen Preparation

Southern yellow pine veneer with dimension of 300 × 300 × 3.5 mm^3 were preconditioned in the 27°C and 30% relative humidity chamber for 7 day prior to the panel assemble. The adhesive was applied to the bottom and top of the center ply only by a brush with spread rate 20–22 g/ft^2, on a wet weight basis. Veneers were oriented in the typical layup, in which the

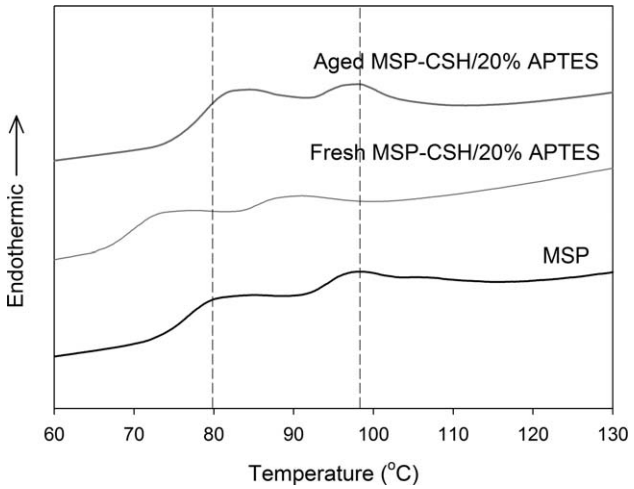

Figure 2. DSC thermograms of MSP and fresh and aged MSP-CSH/20% APTES.

grain of the middle panel is perpendicular to the grain of the top and bottom panels. The assembled three ply veneers were conditioned for 10 min at room temperature, and then hot pressed at 150 psi (1.03 MPa) and 170°C for 10 min.

Shear Strength Measurement

For two ply plywood samples, the assembled wood samples were cooled, conditioned at 23°C and 50% relative humidity for 48 h, and cut into five pieces with dimensions of 80 × 20 mm^2 (glued area of 20 × 20 mm^2). The cut wood specimens were conditioned for another 2 day before measurements were taken. Wood specimens were tested with an Instron Tester (Model 4465, Canton, MA) according to ASTM Standard Method D2339-98[44] at a crosshead speed of 1.6 mm/min. Shear adhesion strength at maximum load was recorded; reported values are the average of four specimen measurements. Water resistance of the wood assemblies was measured following ASTM Standard Methods D1183-96[45] and D1151-00.[46] Six preconditioned specimens were soaked in tap water at 23°C for 48 h, and wet strength was tested immediately after soaking.

For three ply plywood samples, the bonded wood samples were conditioned at 23°C and 50% relative humidity for 48 h before cutting. From each panel, 15 specimens (6 for dry strength and 9 for wet strength) with dimensions of 82.6 × 25.4 mm^2 were obtained according to ASTM Standard Method D 906-98.[47] The cut specimens were conditioned for 48 h, and tested with the same Instron tester at a crosshead speed of 1.0 mm/min. Dry shear adhesion strength at maximum load was recorded; reported values are the average of six specimen measurements. Water resistance of three ply plywood samples was evaluated in terms of wet shear strength. Nine preconditioned specimens (82.6 × 25.4 mm^2) were soaked in water at 23°C for 24 h, and wet strength was tested immediately after soaking.

RESULTS AND DISCUSSION

Thermal Properties

The organic CSH hybrid was synthesized by *in-situ* sol–gel polymerization in which small silicone oxide molecules are converted to an integrated network of polymers and the resulting

Table II. Summary of T_d and ΔT_d of MSP and MSP-CSH Composites with Different Molar Ratios of APTES

MSP/CSH Composites	T_d (°C)		Total (ΔH_d) (J/g)
	7S	11S	
MSP	79.97	97.25	5.62
MSP-CSH	73.01[a]	89.64[a]	5.49
	77.52[b]	93.74[b]	5.58
MSP-CSH/20% APTES	73.21[a]	89.97[a]	5.45
	82.55[b]	98.60[b]	7.80
MSP-CSH/40% APTES	72.82[a]	90.10[a]	5.17
	82.03[b]	98.99[b]	7.14

[a] Temperatures present denaturation temperatures in fresh adhesives.
[b] Temperatures present denaturation temperatures in aged adhesives.

structure changes with aging, producing strengthening, stiffening, or shrinkage of the network. Particularly, the polymerization and solidification of CSH network structure is known to contribute to the mechanical strength of the cement paste after aging.[33,48] For this reason, comparing fresh and aged composites to determine aging effect is critical to observe the interfacial interaction and detailed crosslinking mechanism between soy proteins and CSH. Therefore, aged composites were prepared to store the fresh samples in a plastic container with a lid for 7 days. The DSC thermograms of both fresh and aging composites were collected (Figure 2); data are summarized in Table II.

DSC provides valuable information on unfolding the quaternary, tertiary, and secondary structures of soy protein and subsequent interaction between soy protein and CSH via a crosslinking function of aminopropyl silane (APTES). As shown in Figure 2, MSP has two endothermic transition peaks: One is at 79.97°C from 7S and 97.25°C from 11S for the denaturation peak temperature (T_d) with total enthalpy (ΔH_d) of 5.62 J/g. When MSP-CSH/20% APTES was prepared, the T_d and ΔH_d of the fresh composite decreased, however, they became higher in aged composites with aging effect as shown in Figure 2. Table II summarizes the T_d of 7S and 11S and total ΔH_d in composites

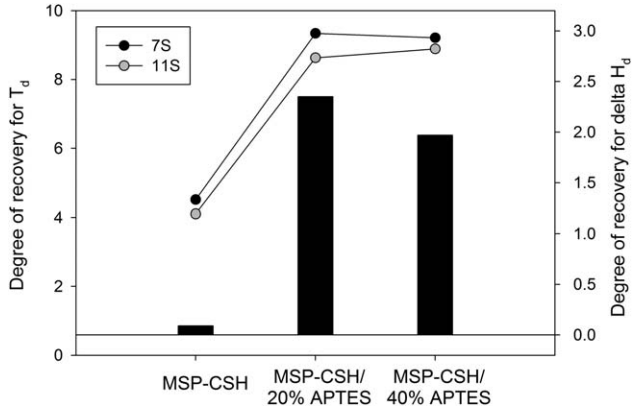

Figure 3. The degree of recovery of T_d and ΔH_d of MSP-CSH composites with different molar ratios of APTES.

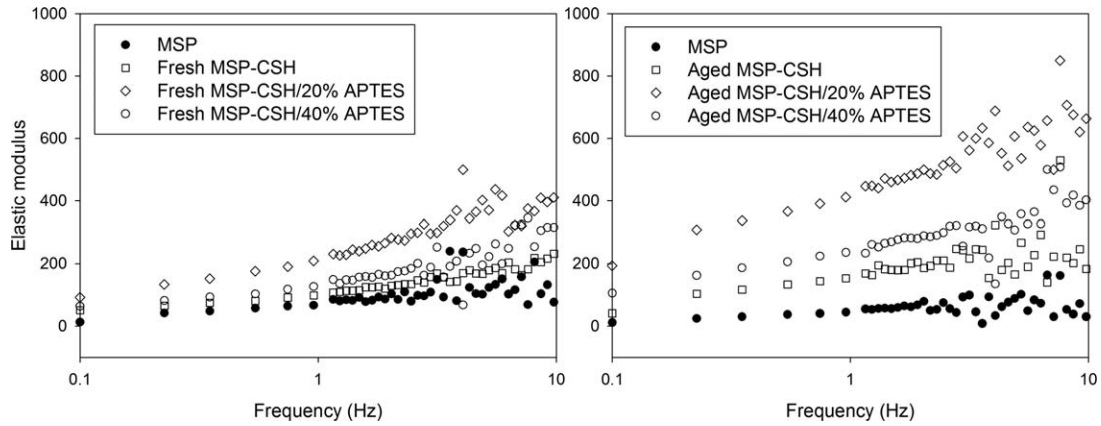

Figure 4. The frequency dependence of the elastic modulus (G') of MSP and MSP-CSH composites with different molar ratios of APTES.

with different molar ratios of APTES. The T_d and ΔH_d of aged composites was higher than for the corresponding fresh ones, representing higher thermal stability. As shown in Table II, the recoveries of T_d and ΔH_d in the MSP-CSH with APTES was significant when APTES was applied as a crosslinking agent, on the other hands, the recovery in MSP-CSH was trivial when the pure CSH (0% APTES, 100% TEOS) was applied.

Less thermal stability in the fresh composites means that the three-dimensional structure of 7S and 11S was affected by the organic CSH hybrid polymerization process. The MSP tends to be additionally unfolded by the byproducts (e.g., ethanol) of the sol–gel reactions during hydrolysis of the organic CSH hybrid. Generally, the organic solvent, such as methanol or ethanol, can denature globular soy proteins by disrupting hydrogen bonds.[49] The ethanol produced in the hydrolysis of silicate precursors can break the intra-or intermolecular interactions within the soy proteins and disrupt the hydrogen bonds, resulting in lower denaturation temperatures for both 7S and 11S in the fresh composites. Moreover, the effect of calcium ionic strength was another possibility to disrupt the three-dimensional structure of protein, resulting in more extensive unfolding of soy protein

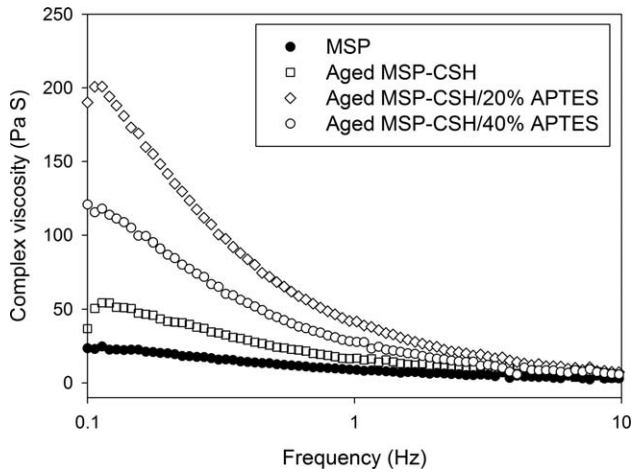

Figure 5. The complex viscosities of MSP and aged MSP-CSH composites with different molar ratios of APTES.

structure with less thermal stability.[50] However, with aging, T_d and ΔH_d of 7S and 11S changed in the aged composites during the interaction between soy protein polymers and CSH via the crosslinking function of APTES. Figure 3 presents the degree of recovery of T_d and ΔH_d in MSP-CSH composites with different molar ratios of APTES. They were calculated by subtracting the T_d and ΔH_d of fresh composites from those of aged ones. As shown in Figure 3, the aged SP-CSH/20% APTES had the largest degree of recovery in T_d and ΔH_d but displayed no increase as the molar ratio of APTES increased further. APTES acts as a crosslinking agent and the unfolded soy proteins could be reassembled through covalent bridges at the interface between soy protein and CSH. With an increasing molar ratio of APTES in the composite, APTES contributed to more crosslinking or grafted reaction between soy polymeric matrix and CSH, showing the higher T_d and ΔH_d. The coupling effect of APTES seemed to level off in the composites; however, when APTES was higher than 20%, which might be due to a random aggregation of silicate precursors in the preparation of organic CSH hybrids. In general, all parameters for sol–gel chemistry significantly affect the gelation time, reaction rate of hydrolysis, and polycondensation and geometry of final silica materials.[51] The molar ratio of the two silica precursors varies in this work and consequently affects the gelation time and rate of aggregation. When CSH/40% APTES was prepared, silica precursors immediately started to aggregate, which could mean lose opportunities for covalent bridges with soy proteins due to such a rapid gelation process. Additionally, the recovery of T_d and ΔH_d was insignificant in MSP-CSH without using a crosslinking agent, confirming that APTES functions as a crosslinking agent between two very different polymer materials. Yet, it still means that unfolded soy proteins also facilitate reassociation with noncovalent interaction based on the small recovery in the aged MSP-CSH (with 0% APTES).

Dynamic Viscoelastic Properties

Upon the *in-situ* polymerization of organic CSH hybrids, a three-dimensional network was formed in the MSP-CSH composites by a crosslinking process. According to thermal properties of MSP-CSH composites, MSP tended to reassemble with

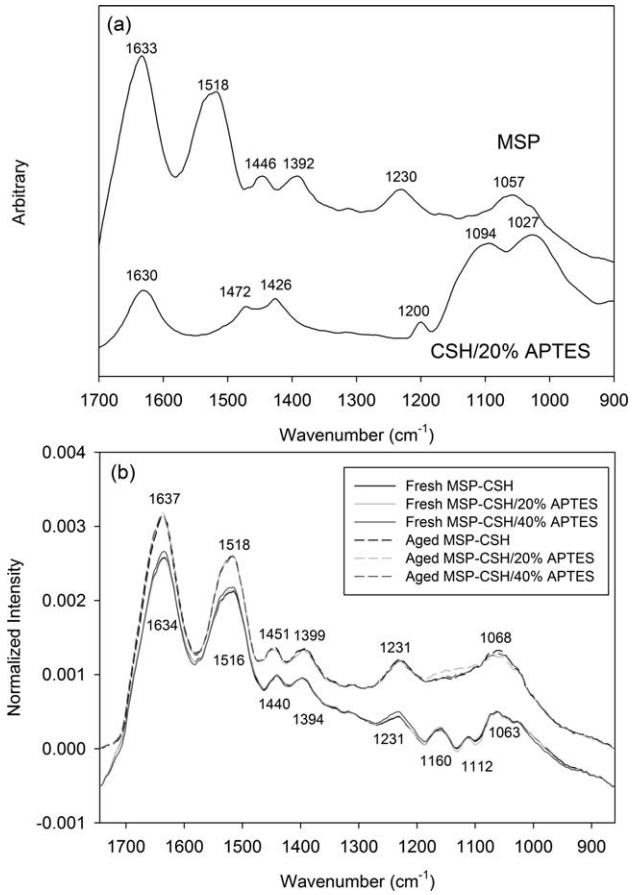

Figure 6. FTIR spectra of (a) MSP and CSH/20% APTES and (b) fresh and aged MSP-CSH composites with different molar ratios of APTES for with spectral ranges from 1700 to 900 cm^{-1}.

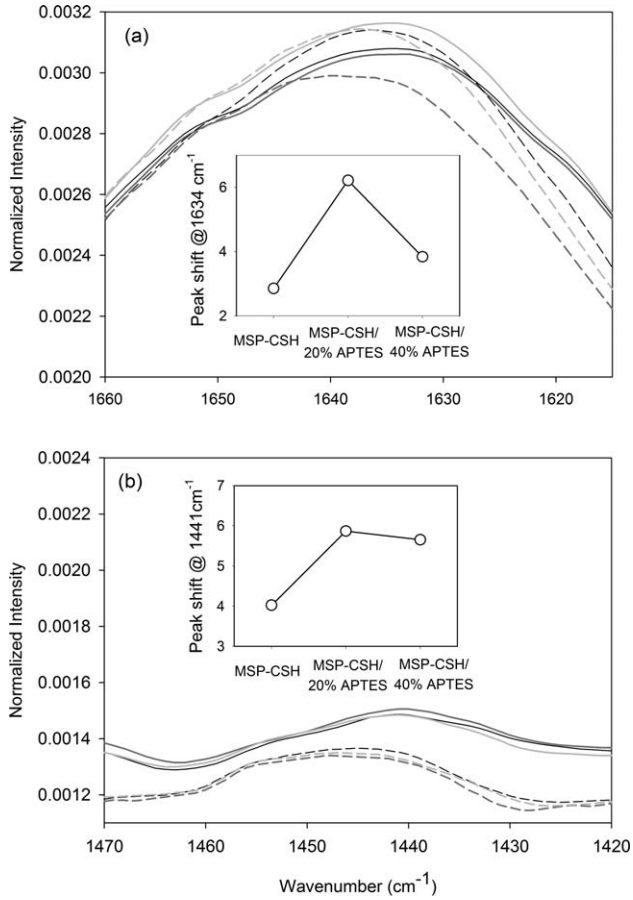

Figure 7. Enlarged spectral feature of peaksand the degree of peak shift at 1634 cm^{-1} (a) and at 1634 cm^{-1} (b) as insets.

covalent and noncovalent interactions in the aged composites, which is expected to possess better adhesion strength.

Dynamic rheological measurement was used to study viscoelastic properties of polymers and was carried out at a small strain within the linear viscoelastic region; the modulus curve was monitored as a function of time and frequency. The elastic modulus of fresh and aged composites is shown in Figure 4. By comparing the elastic modulus of fresh and aged composites, the viscoelastic properties of the MSP-CSH composites changed with aging. Aged composites had higher elastic moduli than fresh ones. The highest elastic modulus was observed in the aged MSP-CSH/20% APTES composite, rather decreased in SP-CSH/40% APTES. MSP-CSH without addition of APTES had almost similar elastic modulus in spite of aging effect. This phenomenon was similar with interpretation of thermal properties. As described earlier, unfolded protein originating from ethanol lead to rearrangement of the protein polymeric matrix and CSH via crosslinking functions, and it is apparent that the grafting silane improves the viscoelastic properties of the MSP-CSH composites. Based on the increase in viscoelastic properties of MSP-CSH composites with aging, we concluded that the crosslinking process of aminopropyl silane occurred between soy proteins and CSH does the rearrangement of protein-protein complex, which lead to the change of rheological properties. Complex viscosities of all aged composites decreased as the frequency increased (Figure 5), revealing a shear thinning behavior. Similarly, the MSP-CSH/20% APTES showed the highest viscosities because of strong intramolecular and intermolecular interactions due to the grafting process of aminopropyl silane. The specific covalent interactions occurring between protein macromolecular chains and organic CSH hybrids resulted in an entangled and interconnected three-dimensional structure in the chemical grafting reaction process.

FTIR Spectroscopic Properties

FTIR spectroscopy was used to identify the conformation change of soy proteins caused by inorganic calcium derivatives and provides supportive evidence for the covalent bonds at the interface between soy proteins and CSH via the crosslinking process of APTES. Figure 6(a) shows the IR spectra of MSP and CSH/20% APTES. The spectrum of MSP shows the main absorption bands of peptide linkage in soy proteins. The peak near 1633 cm^{-1} is the amide I band, which resulted from the C═O stretching vibrations of the peptide bond. Similarly, the peaks near 1518 cm^{-1} (N—H bending vibration/C—N stretching vibration) and 1230 cm^{-1} (C—N stretching vibration/N—H bending vibration) are called the amide II band and amide III band, respectively.[52] The peak near 1392 cm^{-1} resulted from protein side-chain COO^{-}. Furthermore, the stretching C-NH_2 of side-chain primary amines

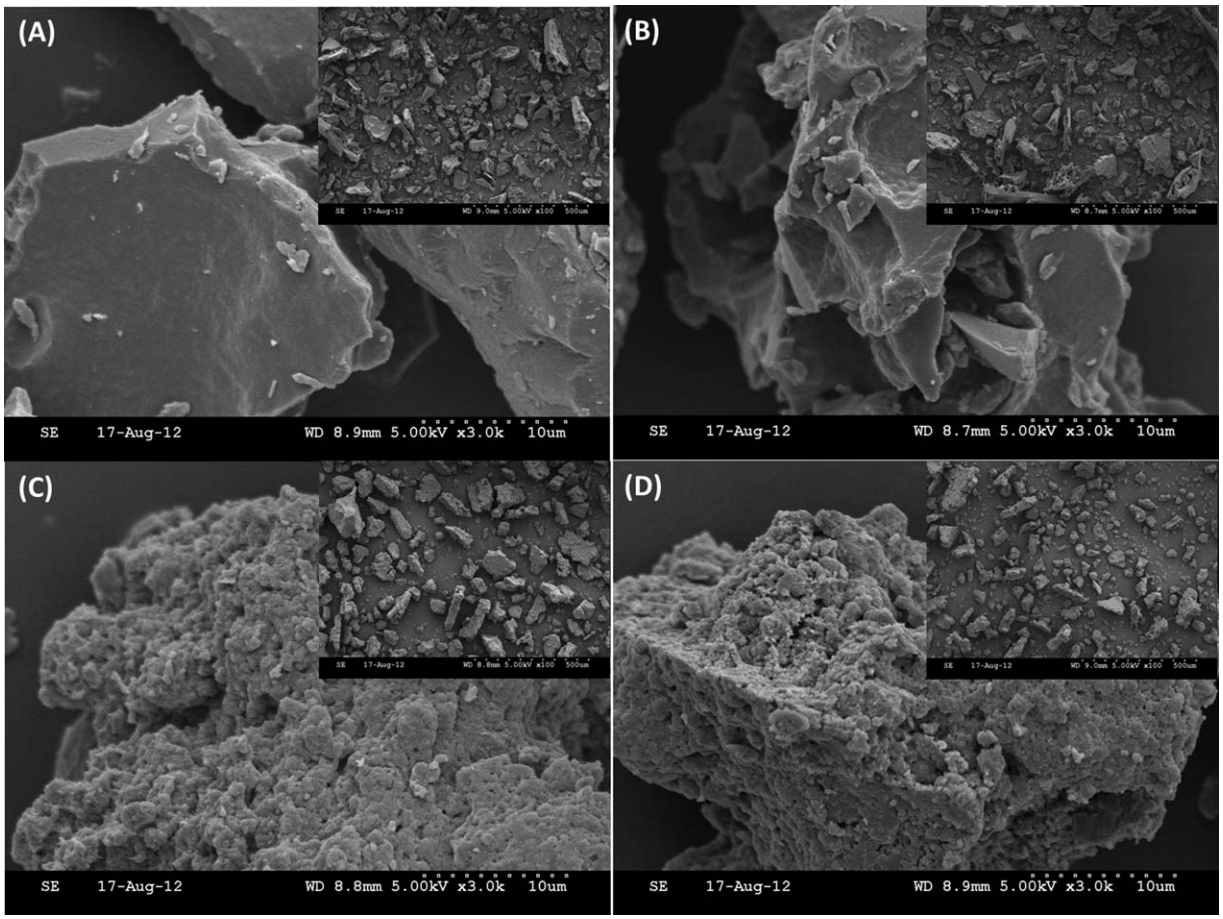

Figure 8. SEM images of MSP-CSH composites with different molar ratios of APTES (a) MSP, (b) MSP-CSH, (c) MSP-CSH/20% APTES, and (d) MSP-CSH/40% APTES.

appeared at 1446 cm^{-1}, and weaker bands related to C—N stretching and bending vibrations of protein backbone and amino acid residues were located at 1057 cm^{-1}.

The spectroscopic samples of CSH/20% APTES were prepared by completing the gelation process at ambient temperature, evaporating all solvent, and then freeze-drying. The spectral region between 1700 and 860 cm^{-1} has several bands whose intensity is mainly due to APTES: δ (NH_2) at 1472 cm^{-1} and $\delta_A(CH_3)$ at 1426 cm^{-1} due to CH_3 and CH_2 bending and stretching of APTES.[53] A strong band of O—H stretching vibration is at 1630 cm^{-1} due to the absorption of atmospheric moisture. The most intensive spectral region is between 1200 and 900 cm^{-1}.The C—N stretching of APTES amino groups is shown at 1200 cm^{-1}. Si—O—C asymmetric stretching occurs at 1094 cm^{-1}, and Si—O—Si symmetric stretching occurs at 1027 cm^{-1}.[53,54] As the molar ratio of APTES varied from 40% to 0%, the ratio of two peaks at 1094 $cm^{-1}$to 1027 cm^{-1} decreased (data not shown).

The spectral range from 1750 to 860 cm^{-1} of both fresh and aged MSP-CSH composites with 0, 20, and 40% APTES are shown in the Figure 6(b). All fundamental structural absorption peaks of MSP still appeared in the spectra of all composites. The strong amide I and II bands appeared in all composites and other spectral features were similar to MSP, except for the spectral range from 1200 to 1000 cm^{-1}. The bands from this range were mostly from Si—O—Si bonds of CSH. In the fresh composites, two bands relating to silicone oxide appeared at 1160 and 1112 cm^{-1}; these bands were shifted compared with those at 1094 and 1027 cm^{-1} of CSH/20% APTES [Figure 6(a)]. This shift indicates that CSH interact with MSP to create *in-situ* polymerization, and these two peaks were integrated and

Table III. Shear Adhesion Strength and Wood Cohesive Failure of MSP-CSH Composites with Cherry Wood

Samples	Dry strength (MPa)	WCF (%)	Wet strength (MPa)	WCF (%)
MSP	2.19 ± 0.22	41.67	1.99 ± 0.39	15.83
MSP-CSH	2.28 ± 0.29	51.67	2.22 ± 0.23	11.67
MSP-CSH/20% APTES	2.73 ± 0.21	60.00	2.44 ± 0.05	23.33
MSP-CSH/40% APTES	2.54 ± 0.25	73.33	2.27 ± 0.13	11.67

Table IV. Shear Adhesion Strength and Wood Cohesive Failure of MSP-CSH Composites with Yellow Pine Wood

Samples	Dry strength (MPa)	WCF (%)	Wet strength (MPa)	WCF (%)
MSP	0.92 ± 0.18	11.25	0.10 ± 0.06	2.86
MSP-CSH	0.86 ± 0.23	18.13	0.47 ± 0.11	18.57
MSP-CSH/20% APTES	1.08 ± 0.18	56.25	0.59 ± 0.20	25.00
MSP-CSH/40% APTES	1.19 ± 0.27	15.63	0.43 ± 0.10	14.00

merged into one broad band with weak intensity, with aging effects as shown in Figure 6(b).

Because the aminopropyl group of APTES mostly overlaps with soy proteins in IR spectral features, a slight change in peak ratio or shift can provide an important clue to explain the crosslinking mechanism at the interface between protein polymers and CSH. Two important peak shifts occurred in the spectral features at 1634 cm^{-1} and 1441cm^{-1}. Figure 7(a) presents the amide I band at 1634 cm^{-1} and the inset shows the degree of the peak shift. The peak shift was calculated by subtracting peak maxima of IR spectra of aged composites from those of fresh ones; they were all blue shifted toward shorter wavelength and higher energy. The degree of the peak shift was the most significant in the aged MSP-CSH/20% APTES, as shown in the inset of Figure 7(a). As described earlier, this peak was a strong typical amide I resulting mainly from C═O stretching. The shift of this peak indicates that possible intra-hydrogen bonding was involved between protein polymers and CSH.[22,55] Soy protein contains many functional groups, including carboxylic (-COOH) and hydroxyl (—OH) acids, which have potential to react with the aminopropyl (-$NH_2(CH_2)_3$—) of APTES. Another interesting point is the peak shift of the adsorption bands at 1441 cm^{-1} with C—NH_2 stretching. All composites demonstrated a blue shift with aging, as depicted in Figure 7(b). Peak maxima were blue shifted with aging effect and the largest shift was observed in aged MSP-CSH/20% APTES. Changes to peak maxima in the aged composites indicate that the crosslinking of APTES occurred at the interface of soy proteins and CSH. The NH_2 of APTES reacted with side chains of soy protein, which was confirmed by the peak shift at C═O stretching at 1634 cm^{-1} and NH_2 stretching at 1441 cm^{-1}. Such a reaction of aminoproply groups of the silicate precursor with side chains of proteins has been observed by IR spectroscopy performed by other researchers.[22]

Morphological Properties

The microstructures of MSP-CSH composites are presented in Figure 8. Pure MSP showed irregular particles with different sizes and smooth surfaces as shown in Figure 8(a). As APTES concentration increased from 0 to 40%, the protein particle surface became more coarse and fluctuant, exhibiting a rough appearance [Figure 8(b–d)]. Pure inorganic CSH is a silica aggregate particle with sizes ranging from approximately 80–300 nm confirmed by transmission electron microscopy. However, the particle surface had big bumps and a little rougher surface in MSP-CSH as shown in Figure 8(b). In addition, the roughness became increased as a mole ratio of APTES was increased in Figure 8(c,d), meaning silica aggregates from inorganic CSH coated the protein surface. As explained previously, MSP is partially unfolded protein and its functional groups can react with APTES coupled to inorganic CSH, displaying reacted rough coatings.

Shear Adhesion Strength

The dry and wet shear adhesion strength of MSP and MSP-CSH composites were evaluated with two types of wood substrates, cherry wood (Table III) and southern yellow pine (Table IV). The dry and wet adhesion strengths of all composites with cherry wood were improved compared with MSP as summarized in Table III. The MSP-CSH/20% APTES has the highest adhesion strength (2.73 MPa for dry and 2.44 MPa for wet strength) and wood cohesive failure (WCF). The crosslinking effect was the most significant in the MSP-CSH/20% APTES, which formed a covalent interface with improved cohesion and adhesion in the MSP-CSH/20% APTES.

Table IV summarizes the shear adhesion strength results of all composites with southern yellow pine. The dry strength increased with the increased molar ratio of APTES from 0.92 to 1.19 MPa, but WCF was highest for the MSP-CSH/20% APTES then decreased for the MSP-CSH/40% APTES. Highest WCF showed the fiber pulled out from the glued wood surface at 20% ATPES mole ratio could be grafted onto some soy protein functional groups, such as COOH and OH, through aminopropyl silane coupling, which could be beneficial to the protein adhesion strength. On the other hand, wet shear adhesion strength of all composites improved significantly compared with MSP. The MSP-CSH/20% APTES showed the most improvement in wet adhesion strength and WCF. Through the reaction between soy protein and CSH to form stable covalent bridges, water-sensitive functional groups were removed and this helps to increase water resistance of the composites.

CONCLUSIONS

We first demonstrated that inorganic CSH formed covalent linkage with soy protein that improved the adhesion strength of soy protein-based composites. The partially unfolded soy protein was reacted with aminopropyl groups of APTES, which was incorporated into inorganic CSH phases. APTES helped to form a crosslinked interface between soy protein and CSH, which was confirmed by FTIR techniques and the changes in thermal, rheological, and morphological properties with aging effect. The entangled and interwoven polymeric structure based on the crosslinked interface promoted the attachment to the solid surface, which consequently leads to the improvement of bonding strength among protein molecules compared to the unmodified soy protein-based adhesives. Therefore, the CSH modified soy protein become more water resistance leading to higher wet adhesion strength.

ACKNOWLEDGMENTS

This work was supported by the NSF EPSCoR Award EPS-0903806 and the Kansas Agricultural Experimental Station with contribution No. 14-031-J.

REFERENCES

1. Peng, I. C.; Quass, D. W.; Dayton, W. R.; Allen, C. E. *Cereal Chem.* **1984**, *61*, 480.
2. Thanh, V. H.; Shibasaki, K. *J. Agric. Food. Chem.* **1978**, *26*, 692.
3. Staswick, P. E.; Hermodson, M. A.; Nielsen, N. C. *J. Biol. Chem.* **1984**, *259*, 3431.
4. Kato, A. *ACS Symp Ser.* **1991**, *454*, 13.
5. Lambuth, A. L. In Handbook of Adhesives, Skeist, I.Ed.; Van Nostrand Reinhold Co.: New York, **1977**, 172–180.
6. Zhong, Z. K.; Sun, X. Z. S. *Polymer* **2001**, *42*, 6961.
7. Hettiarachchy, N. S.; Kalapathy, U.; Myers, D. J. *J. Am. Oil Chem. Soc.* **1995**, *72*, 1461.
8. Wu, W. U.; Hettiarachchy, N. S.; Qi, M. *J. Am. Oil Chem. Soc.* **1998**, *75*, 845.
9. Mackay, K. S. Soybeans and Soybean Products. Vol. II.; Interscience Publishers, Inc.: New York, **1951**.
10. Huang, W. N.; Sun, X. Z. *J. Am. Oil Chem. Soc.* **2000**, *77*, 705.
11. Markley, K. S. **1951**, 621.
12. Chae, H. J.; In, M.; Kim, M. H. *Agric. Chem. Biotechnol.* **1997**, *40*, 404.
13. Hamada, J. S.; Marshall, W. E. *J. Food Sci.* **1989**, *54*, 598.
14. Kalapathy, U.; Hettiarachchy, N.; Myers, D.; Hanna, M. A. *J. Am. Oil Chem. Soc.* **1995**, *72*, 507.
15. Singha, A. S.; Thakur, V. K. *Int. J. Polym. Analy. Characterization* **2010**, *15*, 87.
16. Thakur, V. K.; Singha, A. S.; Mehta, I. K. *Int. J. Polym. Analy. Characterization* **2010**, *15*, 137.
17. Thakur, V. K.; Singha, A. S.; Kaur, I.; Nagarajarao, R. P.; Yang, L. *Int. J. Polym. Anal. Characterization* **2010**, *15*, 397.
18. Singha, A. S.; Thakur, V. K. *Bioresources* **2009**, *4*, 292.
19. Singha, A. S.; Thakur, V. K. *Polym. Compos.* **2010**, *31*, 459.
20. Singha, A. S.; Thakur, V. K. *J. Reinf. Plast. Compos.* **2010**, *29*, 700.
21. Huang, W. N.; Sun, X. Z. *J. Am. Oil Chem. Soc.* **2000**, *77*, 101.
22. Liang, F.; Wang, Y. Proceedings-American Society for Composites Technical Conference; 14th, American Society for Composites **1999**, 14th, 511.
23. Otaigbe, J. *Plast. Eng.* **1998**, *54*, 37.
24. Kalapathy, U.; Hettiarachchy, N. S.; Myers, D.; Rhee, K. C. *J. Am. Oil Chem. Soc.* **1996**, *73*, 1063.
25. Kumar, R.; Choudhary, V.; Mishra, S.; Varma, I. K. *J. Thermal Anal. Calorimetry* **2004**, *75*, 727.
26. Li, K.; Peshkova, S.; Geng, X. *J. Am. Oil Chem. Soc.* **2004**, *81*, 487.
27. Wescott, J. M.; Frihart, C. R.; Traska, A. E. *J. Adhes. Sci. Technol.* **2006**, *20*, 859.
28. Frihart, C. R. *McGraw Hill Yearbook Sci. Technol.* **2010**, *2010*, 354.
29. van der Leeden, M.; Rutten, A.; Frens, G. *J. Biotechnol.* **2000**, *79*, 211.
30. Suzuki, S.; Sinn, E. *J. Mater. Sci. Lett.* **1993**, *12*, 542.
31. Taylor, H. F. W. *J. Am. Ceram. Soc.* **1986**, *69*, 464.
32. Liu, W.; Chang, J. *Mater. Sci. Eng. C-Mater. Biol. Appl.* **2009**, *29*, 2486.
33. Lin, Q.; Lan, X.; Li, Y.; Ni, Y.; Lu, C.; Chen, Y.; Xu, Z. *J. Biomed. Mater. Res. Part B-Appl. Biomater.* **2010**, *95*, 347.
34. Yip, C. K.; Van Deventer, J. S. J. *J. Mater. Sci.* **2003**, *38*, 3851.
35. Liu, W.; Chang, J. *Mater. Sci. Eng. C-Mater. Biol. Appl.* **2009**, *29*, 2486.
36. Mojumdar, S.; Raki, L. *J. Therm. Anal. Calorim.* **2005**, *82*, 89.
37. Minet, J.; Abramson, S.; Bresson, B.; Franceschini, A.; Van Damme, H.; Lequeux, N. *J. Mater. Chem.* **2006**, *16*, 1379.
38. Yang, I.; Kuo, M.; Myers, D. J. *J. Am. Oil Chem. Soc.* **2006**, *73*, 231.
39. Wescott, J. M.; Frihart, C. R. Int. Wood Compos. Mater. Symp Proc. **2004**, 38th, 199.
40. Qi, G. S.; Xiuzhi. *J. Am. Oil Chem. Soc.* **2011**, *88*, 271.
41. Qi, G.; Li, N.; Wang, D.; Sun, X. S. *J. Am. Oil Chem. Soc.* **2012**, *89*, 301.
42. Qi, G.; Li, N.; Wang, D.; Sun, X. S. *Indus. Crops Products* **2013**, *46*, 165.
43. Otaigbe, J. U.; Adams, D. O. *J. Environ. Polym. Degrad.* **1997**, *5*, 199.
44. Anonymous, In Annual Book of ASTM Standards, ASTM International: West Conshohocken, PA, **2002**, 158.
45. Anonymous, In Annual Book of ASTM Standards, ASTM International: West Conshohocken, PA, **2002**, 70.
46. Anonymous, In Annual Book of ASTM Standards, ASTM International: West Conshohocken, PA, **2002**, 67.
47. Anonymous, In Annual Book of ASTM Standards, ASTM International: West Conshohocken, PA, **2002**, 1.
48. Peterson, V. K.; Neumann, D. A.; Livingston, R. A. *Chem. Phys. Lett.* **2006**, *419*, 16.
49. Fukushim, D. *Cereal Chem.* **1969**, *46*, 405.
50. Babajimopoulos, M.; Damodaran, S.; Rizvi, S. S. H.; Kinsella, J. E. *J. Agric. Food. Chem.* **1983**, *31*, 1270.
51. Brinker, C. J.; Scherer, G. W. *J. Non Cryst Solids* **1985**, *70*, 301.
52. Schmidt, V.; Giacomelli, C.; Soldi, V. *Polym. Degrad. Stab.* **2005**, *87*, 25.
53. Pena-Alonso, R.; Rubio, F.; Rubio, J.; Oteo, J. L. *J. Mater. Sci.* **2007**, *42*, 595.
54. Kamnev, A. A.; Dykman, L. A.; Tarantilis, P. A.; Polissiou, M. G. *Met. Ions Biol. Med.* **2002**, *7*, 104.
55. Qi, G.; Sun, X. S. *J. Am. Oil Chem. Soc.* **2011**, *88*, 271.